Solar Energy Materials & Solar Cells 93 (2009) 1230–1237

Contents lists available at ScienceDirect

Solar Energy Materials & Solar Cells

journal homepage: www.elsevier.com/locate/solmat

Preparation and characterization of spray-deposited Cu_2ZnSnS_4 thin films

Y.B. Kishore Kumar, G. Suresh Babu, P. Uday Bhaskar, V. Sundara Raja *

Solar Energy Laboratory, Department of Physics, Sri Venkateswara University, Tirupati 517 502, India

ARTICLE INFO

Article history:
Received 5 April 2008
Received in revised form
30 December 2008
Accepted 18 January 2009
Available online 3 March 2009

Keywords:
Cu_2ZnSnS_4
Thin films
Spray pyrolysis
Characterization
Solar cell absorber

ABSTRACT

Thin films of Cu_2ZnSnS_4 (CZTS), a potential candidate for absorber layer in thin film heterojunction solar cell, have been successfully deposited by spray pyrolysis technique on soda-lime glass substrates. The effect of substrate temperature on the growth of CZTS films is investigated. X-ray diffraction studies reveal that polycrystalline CZTS films with better crystallinity could be obtained for substrate temperatures in the range 643–683 K. The lattice parameters are found to be $a = 0.542$ and $c = 1.085$ nm. The optical band gap of films deposited at various substrate temperatures is found to lie between 1.40 and 1.45 eV. The average optical absorption coefficient is found to be $>10^4\,cm^{-1}$.

1. Introduction

$CuInSe_2$-based chalcopyrite semiconductors have proved to be successful candidates for terrestrial photovoltaics (PV). Cu(In,-Ga)Se_2 (CIGSe) thin film solar cells exhibited a record conversion efficiency of 19.9% [1]. These cells utilize expensive and scarce elements like indium, which affects large-scale production. To achieve the goal of cost-effective photovoltaic technology, it is necessary to explore new materials like $Cu_2ZnSnSe_4$, Cu_2ZnSnS_4 and other quaternaries of these chalcopyrite-like semiconductors. The elements zinc and tin in these compound semiconductors are relatively cheap and abundant compared to indium and gallium used in CIGS thin film solar cells. Cu_2ZnSnS_4 (CZTS), with a direct band gap (1.45 eV) close to optimum value for PV applications, high optical absorption coefficient ($\sim 10^4\,cm^{-1}$) and p-type conductivity is a promising material for absorber layer in thin film solar cells. A thorough understanding of material properties is very much essential for the successful utilization of this compound in solar cells. Only limited work is done on the growth and characterization of CZTS bulk [2–10] and thin films [11–33]. Nitsche et al. [2] had successfully grown Cu_2ZnSnS_4 single crystal in 1967 by vapour-phase iodine transport. Schäfer and Nitsche [3] later reported the structural properties of many Cu_2–II–IV–S_4(Se_4) single crystals. Hall et al. [4] investigated the structural difference between Cu_2(Fe,Zn)SnS_4 and Cu_2(Zn,Fe)SnS_4 using single crystal X-ray diffraction methods. Bernardini et al. [5] carried out EPR and SQUID magnetometry studies on natural and synthetic Cu_2FeSnS_4 (stannite) and Cu_2ZnSnS_4 (kesterite) crystals. Structural investigation of synthetic Cu_2FeSnS_4–Cu_2ZnSnS_4 single crystals was reported by Bonazzi et al. [6]. Mössbauer study on stannite–kesterite solid solutions was investigated by Benedetto et al. [7]. Matsushita et al. [8] carried out X-ray diffraction (XRD) and differential thermal analysis (DTA) studies on Cu_2ZnSnS_4 and other related compound semiconductors synthesized from elemental mixture. Tanaka et al. [9] reported for the first time the photoluminescence studies of CZTS bulk crystals grown by iodine transport method. Recently Schorr et al. [10] reported structural characterization results on stannite–kesterite solid solution series by neutron diffraction studies. Ito and Nakazawa [11] reported for the first time a CZTS/CdSnO heterojunction using CZTS films deposited by sputtering. Friedlmeier et al. [12] investigated the properties of thermally-evaporated CZTS films and reported a CZTS/CdS/ZnO heterojunction with an efficiency of 2.3%. Katagiri and co-workers have extensively investigated CZTS films prepared by sulphurisation of electron beam evaporated [13–20] as well as RF sputtered [21] precursors. CZTS cells with an efficiency of 5.74%, using vapour-phase sulphurized RF sputtered precursors, have been reported in 2007 [22]. Seol et al. [23] investigated electrical and optical properties of RF magnetron sputtered CZTS film. Hybrid sputtering [24], co-evaporation [25], pulsed laser deposition [26] and sulphurisation of metallic/compound precursors deposited using vacuum evaporation [27], ion beam sputtering [28] and sputtering and sequential evaporation [29] have been used in recent years to deposit CZTS films.

Apart from the physical vapour deposition methods cited above for the deposition of CZTS films, chemical deposition methods like photo-chemical deposition [30], sol–gel [31] and spray pyrolysis [32–34] have been used to deposit these films.

* Corresponding author. Tel.: +91 877 2289472; fax: +91 877 2248485.
E-mail address: sundararajav@rediffmail.com (V. Sundara Raja).

0927-0248/$ - see front matter © 2009 Elsevier B.V. All rights reserved.
doi:10.1016/j.solmat.2009.01.011

Table 1
Elemental composition of the CZTS films deposited at different T_s.

Substrate temperature (T_s) (K)	Composition of elements in atomic %				Cu/(Zn+Sn)
	Cu	Zn	Sn	S	
563	27.49	19.43	11.16	41.91	0.90
603	26.86	18.64	13.53	40.96	0.84
643	27.20	18.96	11.31	42.53	0.92
683	28.78	16.99	14.37	39.86	0.92
723	28.58	19.98	15.43	36.01	0.81

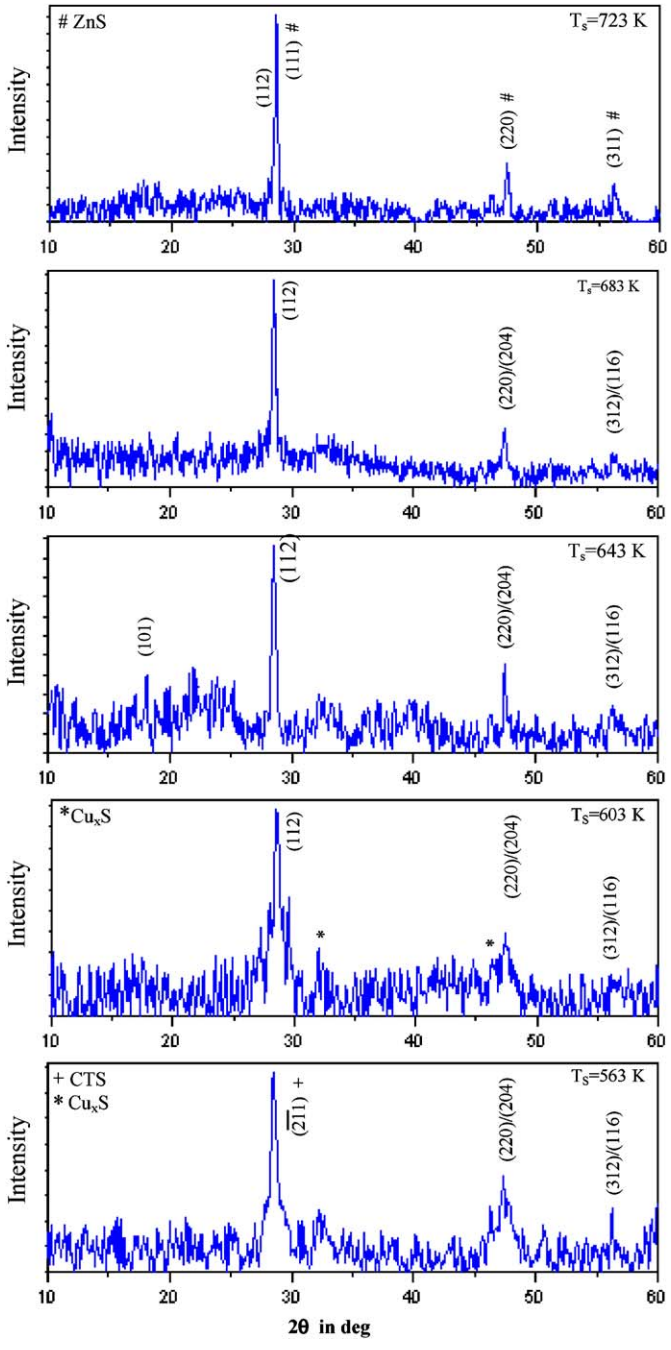

Fig. 1. XRD patterns of CZTS films deposited at different T_s's.

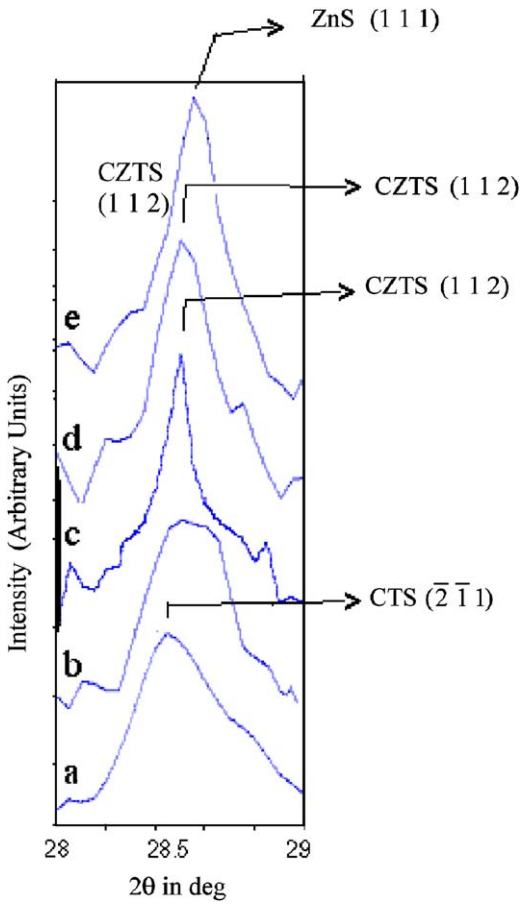

Fig. 2. Expanded view of XRD peaks of CZTS films deposited at (a) 563, (b) 603, (c) 643, (d) 683 and (e) 723 K.

Spray pyrolysis is a versatile and low-cost technique, which is extensively used to deposit selenide, sulphide and oxide semiconductor films. Nakayama and Ito [32] studied the effect of ethanol and zinc concentration in the starting solution on the properties of spray-deposited CZTS films using N_2 as the carrier gas. Films grown from aqueous solution are highly sulphur-deficient (28–30%) and near stoichiometric CZTS films were obtained with a solution containing 30% ethanol. Subsequent annealing of the films in sulphur ambient was found to be necessary. Madarász et al. [33] deposited CZTS films by spray pyrolysis using thiourea complexes but optical and morphological studies were not carried out. Recently Kamoun et al. [34] investigated the effect of substrate temperature (553–633 K) and the spray duration (30, 60 min) on the growth of CZTS films. XRD studies of these films showed that the films are multi-phase. We have investigated the growth and properties of spray-deposited CZTS films at various substrate temperatures in the range 563–723 K in order to optimize substrate temperature to obtain single-phase CZTS films. The results of these investigations are presented in this paper.

2. Experimental

Cu_2ZnSnS_4 thin films were deposited by spray pyrolysis technique starting with an aqueous solution containing cupric chloride (0.01 M), zinc acetate (0.005 M), stannic chloride (0.005 M) and thiourea (0.04 M). Excess thiourea was taken to compensate the loss of sulphur during pyrolysis. The solution was

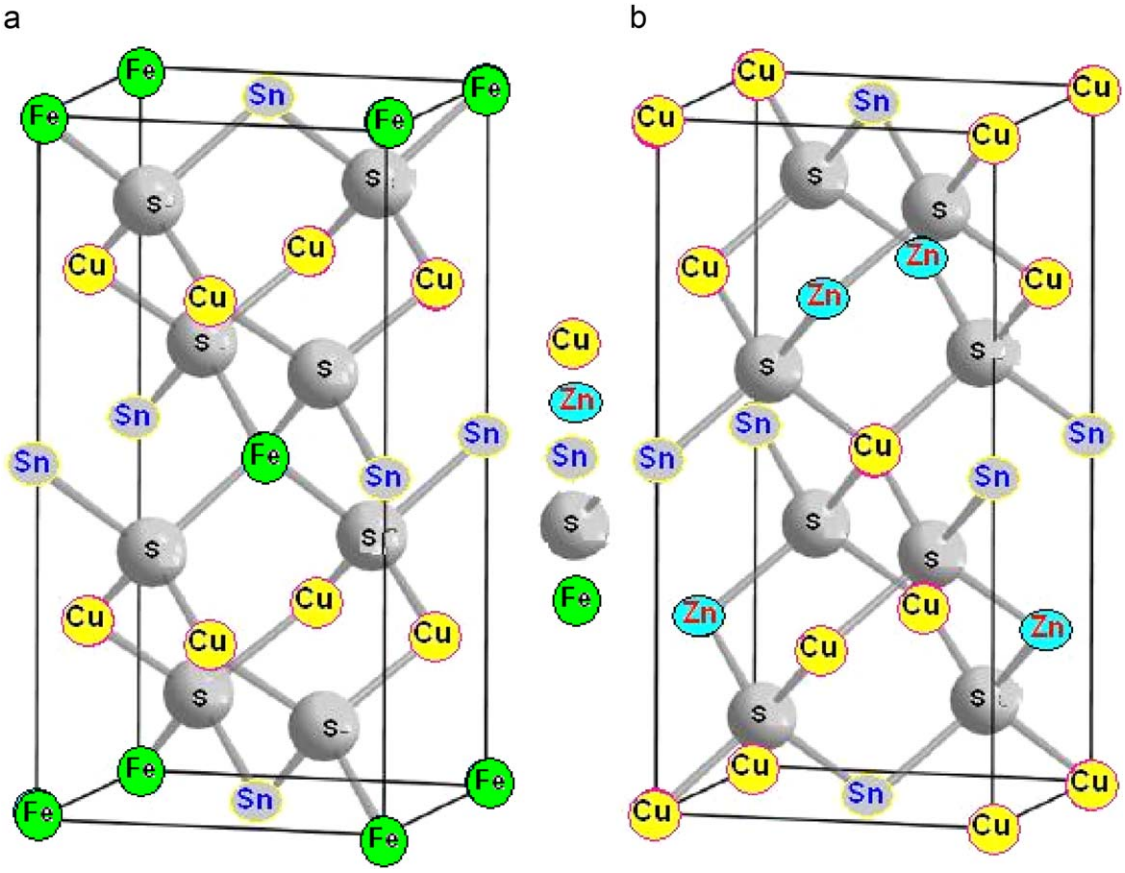

Fig. 3. Crystal structure of (a) mineral stannite (Cu_2FeSnS_4) and (b) mineral kesterite (Cu_2ZnSnS_4).

Table 2
Atomic coordinates positions of elements in stannite (Cu_2FeSnS_4) and kesterite (Cu_2ZnSnS_4) structures [4].

Stannite ($I\bar{4}2\,m$)			Kesterite ($I\bar{4}$)		
Atoms	Wyckoff notation	Position	Atoms	Wyckoff notation	Position
Fe	2a	(0 0 0)	Cu	2a	(0 0 0)
Sn	2b	$(\frac{1}{2}\frac{1}{2}0)$	Sn	2b	$(\frac{1}{2}\frac{1}{2}0)$
Cu	4d	$(0\frac{1}{2}\frac{1}{4})$	Cu	2c	$(0\frac{1}{2}\frac{1}{4})$
S	8i	(x x z)	Zn	2d	$(\frac{1}{2}0\frac{1}{4})$
			S	8g	(x y z)

sprayed, using a pneumatically controlled air-atomizing spray nozzle ($\frac{1}{4}$ JAU, Spraying systems Co., USA), onto heated glass substrates held at various substrate temperatures. Compressed air was used as the carrier gas and the spray rate was 12 ml/min. Experiments were conducted at various substrate temperatures in the range 563–723 K to investigate the effect of substrate temperature (T_s) on the growth of the films. The substrate temperature could be maintained to an accuracy of ± 5 K using a digital temperature controller.

Films were analyzed by studying their composition, structural, optical and electrical properties. X-ray diffractometer (SEIFERT Model 3003 TT) was used in Bragg–Brentano mode to record X-ray diffraction (XRD) patterns. Cu-K_α radiation ($\lambda = 0.15406$ nm) was used to record the spectra in the 2θ range 10–60° with a step size of 0.03°. Spectral transmittance and reflectance were recorded in the wavelength range 300–2000 nm on JASCO UV–VIS–NIR double beam spectrophotometer. The microstructure and the surface morphology were observed using a JEOL scanning electron microscope (SEM). The elemental composition was determined using an energy dispersive spectrometer (EDS) system attached to JEOL SEM. Electrical resistivity of the films at room temperature was determined with a Keithley 617 programmable electrometer.

3. Results and discussion

3.1. Composition

The elemental composition of Cu_2ZnSnS_4 thin films determined from EDS analysis for films deposited at various substrate temperatures is shown in Table 1. There is a considerable deviation from stoichiometry. The films are mostly copper rich, zinc rich but sulphur deficient. Sulphur deficiency is significantly higher at higher substrate temperatures since sulphur is more volatile. Spray-deposited CZTS films obtained from pure aqueous solution by Nakayama and Ito [32] in the substrate temperature range 553–633 K are also sulphur-deficient (28–38 at%). We have taken $CuCl_2$, which is soluble in water as the source of copper instead of CuCl used by them, and there is some improvement in the sulphur content in the film. Yet the films are sulphur-deficient.

3.2. Structural characterization

3.2.1. X-ray diffraction studies

The XRD patterns of CZTS films deposited at different substrate temperatures (563, 603, 643, 683 and 723 K) are shown in Fig. 1. Fig. 2 shows the expanded view of the most intense peak to know

Table 3
Calculated and experimental XRD peak intensities for CZTS thin films.

S. No.	(*h k l*)	*d*-spacing (nm)	Calculated normalized intensity (I/I_0)	Minctryst information card [35]	Experimental intensity
1	(0 0 2)	0.5421	0	0	–
2	(1 0 1)	0.4869	7	4.55	20
3	(1 1 0)	0.3847	2	–	–
4	(1 1 2)	0.3126	100	100	100
5	(1 0 3)	0.3008	2	2	–
6	(2 0 0)	0.2713	5	10.5	–
7	(0 0 4)	0.2714	5	5.22	–
8	(2 0 2)	0.2426	1	–	–
9	(2 1 1)	0.2368	1	–	–
10	(1 1 4)	0.2212	1	–	–
11	(1 0 5)	0.2013	1	–	–
12	(2 2 0)	0.1919	20	18.01	45[a]
13	(2 0 4)	0.1919	40	35.90	45
14	(3 1 2)	0.1636	14	24.73	25
15	(1 1 6)	0.1636	13	12.30	25[a]
16	(3 0 3)	0.1618	0	–	–
17	(2 2 4)	0.1565	4	–	–
18	(3 1 4)	0.1450	2	–	–
19	(0 0 8)	0.1356	3	–	–
20	(3 3 2)	0.1245	5	–	–

[a] (2 2 0)/(2 0 4) and (3 1 2)/(1 1 6) are not resolvable experimentally as $c \sim 2a$.

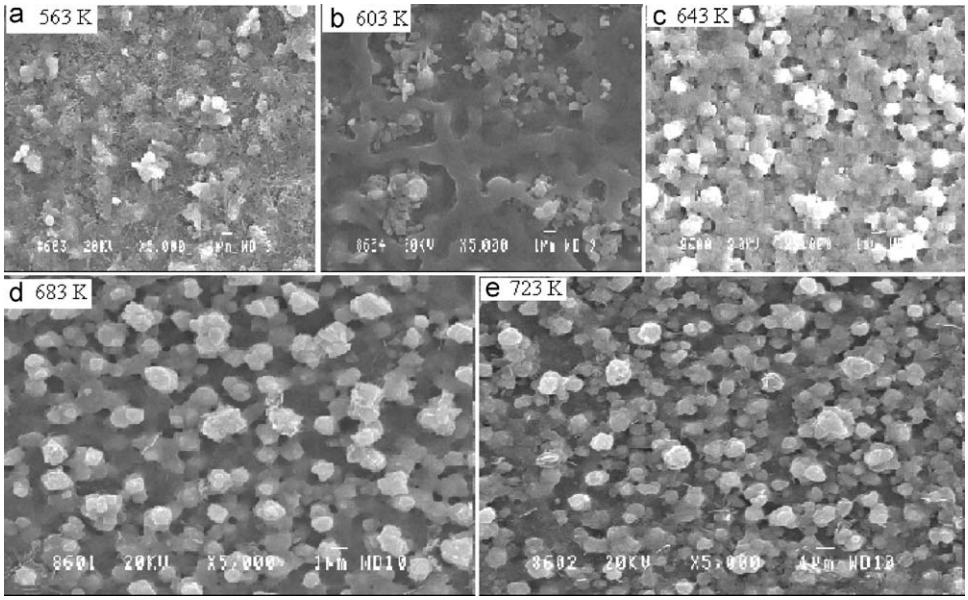

Fig. 4. SEM micrographs of CZTS thin films deposited at (a) 563, (b) 603, (c) 643, (d) 683 and (e) 723 K.

whether peaks corresponding to any secondary phase (Cu_2SnS_3, ZnS) are present. From Fig. 1, it is observed that films deposited at $T_s = 563$ K are multi-phase containing Cu_2SnS_3 (JCPDS Card no. 27-0198), Cu_2ZnSnS_4 and Cu_xS (JCPDS Card no.20-0365) of which Cu_2SnS_3 (CTS) is the dominant secondary phase as indicated by the intense $(\bar{2}\,\bar{1}\,1)$ peak. CZTS films deposited at $T_s = 603$ K are found to contain very weak peaks corresponding to Cu_xS (Fig. 1). XRD patterns of films deposited at $T_s = 643$ and 683 K seem to indicate that the films are single phase since no peak corresponding to any secondary phase is seen. But the low intensity of XRD patterns and considerable deviation from the stoichiometry of these films (Table 1) suggest the possibility of amorphous phases being present in these films. The samples being zinc-rich (Cu/Zn+Sn = 0.92, Zn/Sn = 1.68 and 1.18), ZnS might be present in amorphous form. This proposition might be justified by the fact that films deposited at $T_s = 723$ K are found to contain ZnS as dominant phase possibly due to the improvement in crystallinity at higher T_s (Figs. 1 and 2). The lattice parameters of CZTS films determined from the observed $d_{(1\,1\,2)}$ and $d_{(2\,2\,0)}$ spacings are $a = 0.542 \pm 0.001$ and $c = 1.085 \pm 0.001$ nm. These are in good agreement with the reported single crystal data, $a = 0.5427$ and $c = 1.0848$ nm [3].

There are conflicting reports with regard to the structure of CZTS films. A few groups reported the structure of CZTS films to be stannite [11–13,27–30], while some other groups reported kesterite structure for CZTS films [16,22–26]. Stannite (Cu_2FeSnS_4) and kesterite (Cu_2ZnSnS_4) belong to tetragonal system but the space groups are different. Stannite structure space group is $I\bar{4}2\,m$ while kesterite structure space group is $I\bar{4}$ (Fig. 3). The coordinate positions are shown in Table 2 [4]. However, based on neutron

diffraction studies of stannite–kesterite solid solution series ($Cu_2Fe_{1-x}Zn_xSnS_4$), Schorr et al. [10] recently reported that the structure of Cu_2ZnSnS_4 ($x = 1$ in the series) is unambiguously kesterite ($I\bar{4}$).

We have calculated the intensities of possible diffraction peaks (I_{hkl}) using the atomic scattering factors, coordinate positions and experimentally determined lattice constants a and c values using the formula [36].

$$I_{h\,k\,l} = |F_{h\,k\,l}|^2 P \left[\frac{1+\cos^2 2\theta}{\sin^2\theta \cos\theta}\right] e^{-2M} \quad (1)$$

Here F_{hkl} is structure factor, P is multiplicity factor, M is the temperature factor and θ is the Bragg angle. In the above equation, trigonometric term relates to Lorentz-polarization factor.

The structure factor is given by the equation $F_{hkl} = \sum f_n e^{2\pi i\ (hu+kv+lw)}$ where f_n is atomic scattering factor, (u, v, w) are the coordinates of each atom. The calculated peak intensities for kesterite structure are compared with the normalized experimental peak intensities in Table 3 along with Mincryst information card data [35] for kesterite ($I\bar{4}$). The agreement is reasonably satisfactory. The peak at $d = 0.1919$ nm is assigned to (2 2 0)/(2 0 4). The XRD peaks (2 2 0) and (2 0 4) are not resolvable experimentally as $c \sim 2a$. Similarly, the peaks (3 1 2) and (1 1 6) are also not resolvable. Hence the observed peak at $d = 0.1636$ nm is assigned to (3 1 2)/(1 1 6).

The crystallite size (L) in these films is determined using Scherer's formula [36]

$$L = s\lambda/B\,\mathrm{Cos}\,\theta$$

where s is the Scherer's constant, B is the full-width at half maximum (FWHM) and θ is the Bragg angle. The calculated crystallite size values are found to lie in the range 20–45 nm based on the substrate temperature. The crystallite size is found to increase with increase in substrate temperature.

3.2.2. Microstructure

Fig. 4 shows SEM micrographs of CZTS films deposited at different substrate temperatures. As the substrate temperature increases, there is an improvement in grain morphology and size. Films deposited at $T_s = 563$ K do not exhibit well-defined grains and the appearance is smeary. As T_s increases, the morphology is found to improve and distinct grains are seen for films deposited at $T_s = 683$ and 723 K. The grain size of films deposited for T_s in the range 643–723 K is found to be ~1 μm. It may be worth mentioning here that Scherer's formula gives the crystallite size normal to the X-ray beam direction and does not give lateral dimension [37].

3.3. Optical properties

The optical absorption coefficient (α) was determined from the measured spectral transmittance (T_λ) and reflectance (R_λ) using the formula [38]

$$\alpha t = \ln\left[\frac{(1-R_\lambda)^2}{T_\lambda}\right] \quad (2)$$

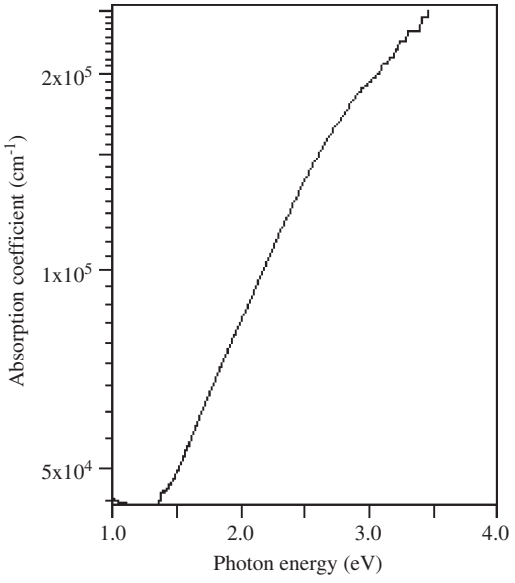

Fig. 5. Optical absorption coefficient of CZTS thin films deposited at $T_s = 643$ K.

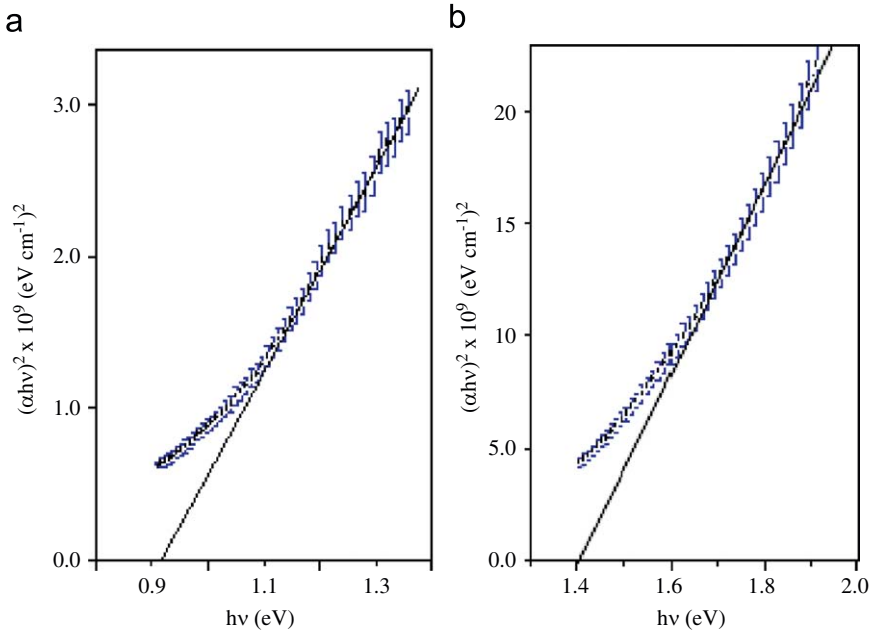

Fig. 6. $(\alpha h\nu)^2$ as a function of photon energy ($h\nu$) for films deposited at $T_s = 563$ K for two different photon energy regions.

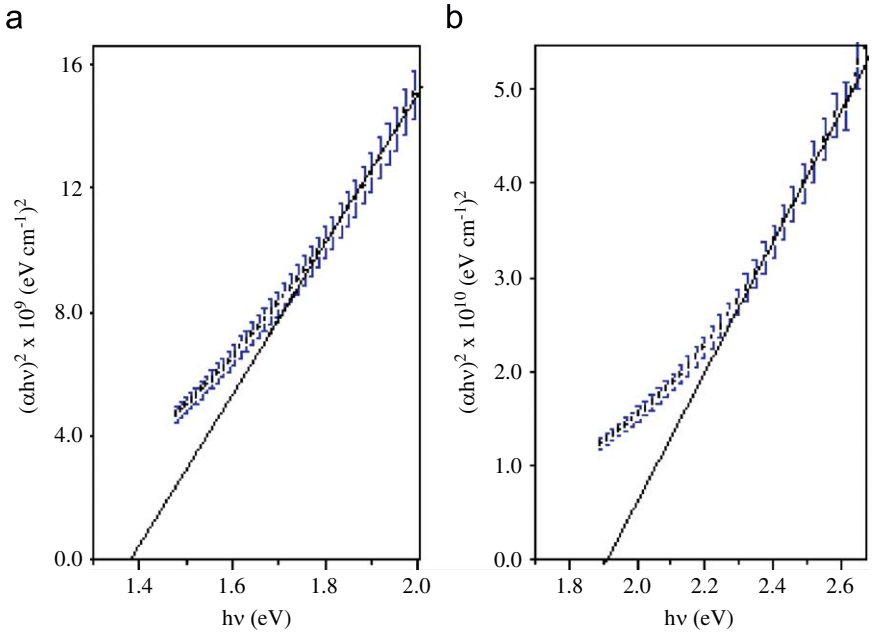

Fig. 7. $(\alpha h\nu)^2$ as a function of photon energy ($h\nu$) for films deposited at $T_s = 603$ K for two different photon energy regions.

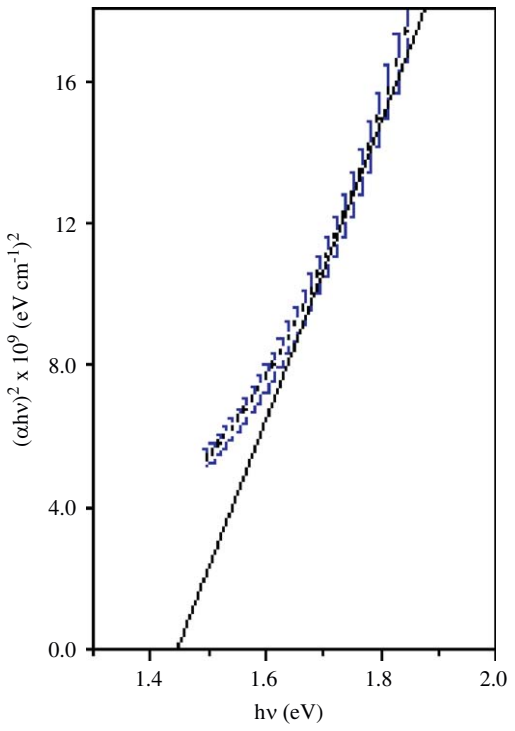

Fig. 8. $(\alpha h\nu)^2$ as a function of photon energy ($h\nu$) for films deposited at $T_s = 643$ K.

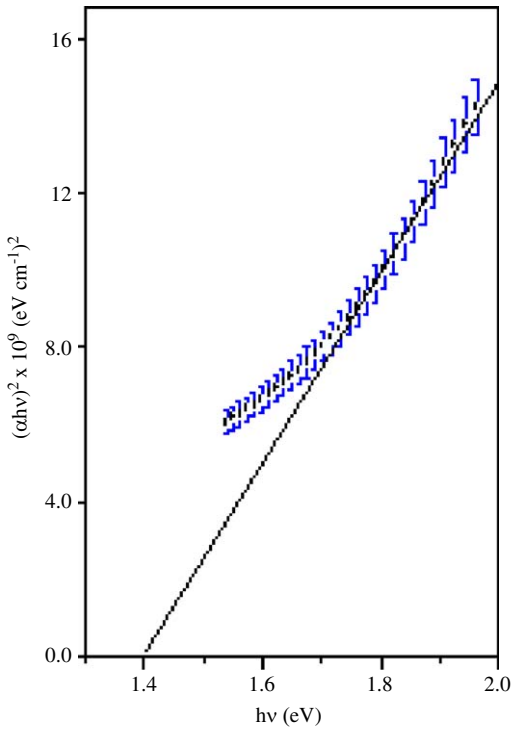

Fig. 9. $(\alpha h\nu)^2$ as a function of photon energy ($h\nu$) for films deposited at $T_s = 683$ K.

where t is the film thickness. A typical plot of optical absorption coefficient versus photon energy ($h\nu$) for films deposited at $T_s = 643$ K is shown in Fig. 5. The nature of the optical transition, whether direct or indirect and the optical band gap (E_g) of each film, is obtained from the equation [38]

$$\alpha = A(h\nu - E_g)^n / h\nu \quad (3)$$

where A is a constant. The exponent 'n' can take values $\frac{1}{2}$, $^3/_2$ or 2 based on whether the optical transition is direct-allowed, direct-allowed or indirect-allowed, respectively. In the present investigation, values of α are found to obey Eq. (3) for $n = \frac{1}{2}$ indicating that the optical transition is direct-allowed in nature. Fig. 6(a) and (b) show the plots of $(\alpha h\nu)^2$ versus $h\nu$ for two different photon energy regions for films deposited at $T_s = 563$ K. The optical band gap values are found to be 0.92 and 1.40 eV, respectively. The uncertainty in the determination of band gap is ± 0.02 eV. The direct optical band gap of 0.92 eV is attributed to Cu_2SnS_3 and 1.40 eV is attributed to CZTS film [11,14]. This

observation that the films contain the secondary phase Cu_2SnS_3 is in agreement with the conclusion from XRD pattern of the films deposited at $T_s = 563$ K. Figs. 7(a) and (b) show the $(\alpha h\nu)^2$ versus plots for two different photon energy regions for the films deposited at $T_s = 603$ K. The direct optical band gap values are found to be 1.39 and 1.90 eV. The former is attributed to direct optical band gap of CZTS and the latter to Cu_xS. The direct optical band gap of Cu_xS reported earlier in the literature is found to vary from 1.7 to 2.16 eV based on the value of x [39]. XRD analysis of the films deposited at $T_s = 603$ K confirmed the presence of CZTS and Cu_xS. The $(\alpha h\nu)^2$ versus $h\nu$ plots for films deposited at $T_s = 643$ and 683 K are shown in Figs. 8 and 9. The direct optical band gaps are found to be 1.45 and 1.40 eV, respectively and are in close agreement with the reported value of CZTS [11,14]. The difference in direct optical band gap values of CZTS films deposited at various substrate temperatures might be due to the difference in the film composition. No other optical transition corresponding to any secondary phase could be noticed in the spectral transmittance curves for these films deposited at $T_s = 643$ and 683 K, indicating that the films are single-phase CZTS. However as stated earlier, considerable deviation of these films (Table 1) from stoichiometry suggests the possibility of amorphous phases being present. The sample being zinc-rich, ZnS might be present in the film. However, the corresponding optical transition could not be observed in the transmittance spectrum owing to the too low spectral intensity below the 500 nm region after strong absorption by CZTS.

3.4. Electrical properties

Room-temperature electrical resistivity of CZTS films deposited at different substrate temperatures was determined using van der Pauw technique. The films were found to be p-type and the resistivity was found to vary from 0.02 to 2.00 Ω cm.

4. Conclusions

Cu_2ZnSnS_4 thin films could be successfully deposited by spray pyrolysis technique. The effect of substrate temperature (T_s) on the growth of spray-deposited Cu_2ZnSnS_4 thin film was investaged. Films deposited at $T_s = 563$ K are found to contain Cu_2SnS_3 and Cu_xS as the secondary phase while at $T_s = 603$ K, Cu_xS is found to be the secondary phase. At $T_s = 723$ K, ZnS appears as the secondary phase. Polycrystalline Cu_2ZnSnS_4 thin films, with amorphous ZnS being present to a small extent, could be obtained in the substrate temperature range 643–683 K. The films exhibited kesterite structure (space group $I\bar{4}$) with lattice parameters $a = 0.542$ and $c = 1.085$ nm. The direct optical band gap of CZTS films deposited under optimized conditions is found to lie between 1.40 and 1.45 eV. Efforts are underway to improve stoichiometry of CZTS films by annealing these films in the presence of sulphur. CZTS films with band gap close to the ideal band gap for highest theoretical conversion efficiency, with an optical absorption coefficient of $>10^4\,cm^{-1}$ and with p-type electrical conductivity could be obtained.

References

[1] Ingrid Repinsl, Miguel A. Contreras, Brain Egaas, Clay DeHart, John Scharf, Craig L. Perkins, Bobby To and Romenel Noufi, 19.9%-efficient ZnO/CdS/CuInGaSe$_2$ solar cell with 81.2% fillfactor, Prog. Photovoltaics: Res. Appl. 16 (2008) 235–239.

[2] R. Nitsche, D.F. Sargent, P. Wild, Crystal growth of quaternary 1_2246_4 chalcogenideds by iodine vapor transport, J. Cryst. Growth (1967) 52–57.

[3] W. Schäfer, R. Nitsche, Tetrahedral quaternary chalcogenides of the type Cu_2–II–IV–S_4 (Se_4), Mater. Res. Bull. 9 (1974) 645–654.

[4] S.R. Hall, J.T. Szymanski, J.M. Stewart, Kesterite, Cu_2(Zn,Fe)SnS_4 and stannite, Cu_2(Fe,Zn)SnS_4 structural similar but distinct minerals, Can. Miner. 16 (1978) 131–137.

[5] G.P. Bernardini, D. Borrini, A. Caneschi, F. Di Benedetto, D. Gatteschi, S. Ristori, M. Romanelli, EPR and SQUID magnetometry study of Cu_2FeSnS_4 (stannite) and Cu_2ZnSnS_4 (kesterite), Phys. Chem. Miner. 27 (2000) 453–461.

[6] P. Bonazzi, L. Bindi, G.P. Bernardini, S. Menchetti, A model for the mechanism of incorporation of Cu, Fe and Zn in the stannite–kësterite series, Cu_2FeSnS_4–Cu_2ZnSnS_4, Can. Miner. 41 (2003) 639–647.

[7] F. Di Benedetto, G.P. Bernardini, D. Borrini, W. Lottermoser, G. Tippelt, G. Amthauer, ^{57}Fe and ^{119}Sn Mössbauer study on stannite (Cu_2FeSnS_4)–kesterite (Cu_2ZnSnS_4) solid solution, Phys. Chem. Miner. 31 (2005) 683–690.

[8] H. Matsushita, T. Maeda, A. Katsui, T. Takizawa, Thermal analysis and synthesis from the metals of Cu-based quaternary compounds Cu–III–IV–VI_4 and Cu_2–II–IV–VI_4, J. Cryst. Growth 208 (2000) 416–422.

[9] K. Tanaka, Y. Miyamoto, H. Uchiki, K. Nakazawa, H. Araki, Donor–acceptor pair recombination luminescence from Cu_2ZnSnS_4 bulk single crystals, Phys. Status Solidi (A) 203 (2006) 2891–2896.

[10] S. Schorr, H.-J. Hoebler, M. Tovar, A neutron diffraction study of the stannite–kesterite solid solution series, Eur. J. Miner. 19 (2007) 65–75.

[11] K. Ito, T. Nakazawa, Electrical and optical properties of stannite-type quaternary semiconductor thin films, Jpn. J. Appl. Phys. 27 (1988) 2094–2097.

[12] Th.M. Friedlmeier, N. Wieser, Th. Walter, H. Dittrich, H.W. Schock, Heterojunctions based on Cu_2ZnSnS_4 and $Cu_2ZnSnSe_4$ thin films, in: Proceedings of the 14th European PVSEC and Exhibition, 1997, P4B.10.

[13] H. Katagiri, N. Sasaguchi, S. Hando, S. Hoshino, J. Ohashi, T. Yokota, Preparation and evaluation of Cu_2ZnSnS_4 thin films by sulfurization of E-B evaporated precursors, in: Technical Digest of the 9th International PVSEC—Miyazaki, Japan, 1996, pp. 745–746.

[14] H. Katagiri, N. Sasaguchi, S. Hando, S. Hoshino, J. Ohashi, T. Yokota, Preparation films by and evaluation of Cu_2ZnSnS_4 thin films by sulfurization of E–B evaporated precursors, Sol. Energy Mater. Sol. Cells 49 (1997) 407–414.

[15] H. Katagiri, N. Ishigaki, T. Ishida, Characterization of Cu_2ZnSnS_4 thin films prepared by vapor phase sulfurization, in: Proceedings of the WCPEC-2, Vienna, Austria, 1998, pp. 640–643.

[16] H. Katagiri, K. Saitoh, T. Washio, H. Shinoham, T. Kurumadani, S. Mivaiima, Development of thin film solar cell based on Cu_2ZnSnS_4 thin films, in: Technical Digest of the 11th International PVSEC, Hokkaido, Japan, 1999, pp. 647–648.

[17] H. Katagiri, N. Ishigaki, T. Ishida, K. Saito, Characterization of Cu_2ZnSnS_4 thin films prepared by vapor phase sulfurization, Jpn. J. Appl. Phys. 40 (2001) 500–504.

[18] H. Katagiri, K. Saito, T. Washio, H. Shinohara, T. Kurumadani, S. Miyajima, Development of thin film solar cell based on Cu_2ZnSnS_4 thin film, Sol. Energy Mater. Sol. Cells 65 (2001) 141–148.

[19] T. Kobayashi, K. Jimbo, K. Tsuchida, S. Shinoda, T. Oyanagi, H. Katagiri, Investigation of Cu_2ZnSnS_4-based thin film solar cells using abundant materials, Jpn. J. Appl. Phys. 44 (2005) 783–787.

[20] H. Katagiri, Cu_2ZnSnS_4 thin film solar cells, Thin Solid Films 480–481 (2005) 426–432.

[21] H. Katagiri, K. Jimbo, K. Moriya, K. Tsuchida, Solar cell without environmental pollution by using CZTS thin film, in: Proceedings of the 3rd World Conference on Photovoltaic Energy Conversion, Oseka, 2003, pp. 2874–2879.

[22] K. Jimbo, R. Kimura, T. Kamimura, S. Yamada, W. Maw, H. Araki, K. Oishi, H. Katagiri, Cu_2ZnSnS_4-type thin film solar cells using abundant materials, Thin Solid Films 515 (2007) 5997–5999.

[23] J. Seol, S. Lee, J. Lee, H. Nam, K. Kim, Electrical and optical properties of Cu_2ZnSnS_4 thin films prepared by rf magnetron sputtering process, Sol. Energy Mater. Sol. Cells 75 (2003) 155–162.

[24] T. Tanaka, T. Nagatomo, D. Kawasaki, M. Nishio, Q. Guo, A. Wakahara, A. Yoshida, H. Ogawa, Preparation of Cu_2ZnSnS_4 thin films by hybrid sputtering, J. Phys. Chem. Solids 66 (2005) 1978–1981.

[25] T. Tanaka, D. Kawasaki, M. Nishio, Q. Guo, H. Ogawa, Fabrication of Cu_2ZnSnS_4 thin films by co-evaporation, Phys. Status Solidi (C) 3 (2006) 2844–2847.

[26] K. Sekiguchi, K. Tanaka, K. Moriya, H. Uchiki, Epitaxial growth of Cu_2ZnSnS_4 thin films by pulsed laser deposition, Phys. Status Solidi (C) 3 (2006) 2618–2621.

[27] L. Shao, Y. Fu, J. Zhang, D. He, Electrical and optical properties of Cu_2ZnSnS_4 thin films prepared for solar cell absorber, Chin. J. Semicond. 28 (2007) 337–340.

[28] J. Zhang, L. Shao, Y. Fu, E. Xie, Cu_2ZnSnS_4, thin films prepared by sulfurization of ion beam sputtered precursor and their electrical and optical properties, Rare Met. 25 (2006) 315–319.

[29] A. Weber, I. Kötschau, S. Schorr, H.-W. Schock, Formation of Cu_2ZnSnS_4 and Cu_2ZnSnS_4-$CuInS_2$ thin films investigated by in-situ energy dispersive X-ray diffraction, Mater. Res. Soc. Symp. Proc. 1012 (2007) 201–208.

[30] K. Moriya, J. Watabe, K. Tanaka, H. Uchiki, Characterization of Cu_2ZnSnS_4 thin films prepared by photo-chemical deposition, Phys. Status Solidi (C) 3 (2006) 2848–2852.

[31] K. Tanaka, N. Moritake, H. Uchiki, Preparation of Cu_2ZnSnS_4 thin films by sulfurizing sol–gel deposited precursors, Sol. Energy Mater. Sol. Cells 91 (2007) 1199–1201.

[32] N. Nakayama, K. Ito, Sprayed films of stannite Cu_2ZnSnS_4, Appl. Surf. Sci. 92 (1996) 171–175.

[33] J. Madarász, P. Bombicz, M. Okuya, S. Kaneko, Thermal decomposition of thiourea complexes of Cu(I), Zn(II) and Sn(II) chlorides as precursors for the spray pyrolysis deposition of sulfide thin films, Solid State Ionics 141–142 (2001) 439–446.
[34] N. Kamoun, H. Bouzouita, B. Rezig, Fabrication and characterization of Cu_2ZnSnS_4 thin films deposited by spray pyrolysis technique, Thin Solid Films 515 (2007) 5949–5952.
[35] Mincryst information card—KESTERITE (Card no. 2333) 〈http://database.iem.ac.ru/mincryst/s_carta.php?KESTERITE〉.
[36] B.D. Cullity, Elements of X-ray Diffraction, Addison-Wesley, London, 1978, pp. 81–143.
[37] H.P. Klug, L.E. Alexander, X-ray Diffraction Procedures, John Wiley and Sons, New York, 1954, pp. 491–538.
[38] I.V. Pankove, Optical Processes in Semiconductors, Dover Inc., New York, 1975, pp. 34–95.
[39] A.C. Rastogi, S. Salkalachen, Optical absorption behaviour of evaporated Cu_xS thin films, Thin Solid Films 97 (1982) 191–199.